CRISPR

RNA-mediated CRISPR-Cas13 inhibition through crRNA structural mimicry

Victoria M. Hayes[1]†, Jun-Tao Zhang[2]†, Mark A. Katz[1], Yuelong Li[2], Benjamin Kocsis[1], David M. Brinkley[1], Ning Jia[2,3]*, Alexander J. Meeske[1]*

To circumvent CRISPR-Cas immunity, phages express anti-CRISPR factors that inhibit the expression or activities of Cas proteins. Whereas most anti-CRISPRs described to date are proteins, recently described small RNAs called RNA anti-CRISPRs (rAcrs) have sequence homology to CRISPR RNAs (crRNAs) and displace them from cognate Cas nucleases. In this work, we report the discovery of rAcrVIA1—a plasmid-encoded small RNA that inhibits the RNA-targeting CRISPR-Cas13 system in its natural host, *Listeria seeligeri*. We solved the cryo–electron microscopy structure of the Cas13-rAcr complex, which revealed that rAcrVIA1 adopts a fold nearly identical to crRNA despite sharing negligible sequence similarity. Collectively, our findings expand the diversity of rAcrs and reveal an example of immune antagonism through RNA structural mimicry.

Bacteriophage and foreign genetic elements subvert CRISPR immunity by producing anti-CRISPRs (Acrs), which inhibit Cas nucleases to enable invasion (*1*). Because Cas nucleases are extremely diverse in sequence, the spectrum of inhibition by a given Acr is typically limited to a single CRISPR type. Although most identified Acrs are proteins, small RNA anti-CRISPRs (rAcrs) inhibit the DNA-targeting type I-C, I-E, I-F, and V-A CRISPR systems (*2*). Owing to their strong resemblance to CRISPR RNAs (crRNAs) in sequence, bioinformatic efforts have identified predicted rAcrs for five of the six major CRISPR types. However, whether additional noncoding RNAs play roles in antagonism of prokaryotic immune systems remains unclear. Furthermore, the structural mechanisms underlying CRISPR-Cas inhibition by rAcrs have not been explored.

A noncoding RNA inhibits CRISPR-Cas13 target interference

The CRISPR-Cas13 inhibitor AcrVIA2 is encoded as part of a 14-kb *acr* locus within an integrated plasmid in *Listeria seeligeri* strain LS21 (Fig. 1A and fig. S1A) (*3*). We introduced a plasmid-borne copy of *acrVIA2* into *L. seeligeri* strain LS1 and tested its ability to inhibit Cas13-mediated restriction of a targeted plasmid (Fig. 1B). When we initially cloned the *acrVIA2* gene, we included the 140–base pair (bp) intergenic region separating it from the upstream gene (Fig. 1A). Although this construct inhibited plasmid targeting by Cas13, introduction of an early stop codon in the *acrVIA2* coding sequence did not diminish the inhibitory effect (Fig. 1B). When we truncated the intergenic region to retain only the 18 bp immediately upstream of the *acrVIA2* start codon, the construct still displayed Cas13 inhibition, but this was abolished upon introduction of the same nonsense mutation (Fig. 1B). Accordingly, we tested a construct containing the 140-bp intergenic region along with only the first 50 bp of the *acrVIA2* coding sequence, which exhibited potent Cas13 inhibition (Fig. 1B). Collectively, these results indicate that an *acr* locus of *L. seeligeri* strain LS21 harbors two adjacent Cas13 inhibitors: one encoded by the *acrVIA2* gene and another encoded just upstream of it.

The 140-bp region between *acrVIA2* and its upstream gene does not encode any predicted open reading frames (ORFs), and constructs in which the AcrVIA2 coding sequence was truncated to 10 bp, contained frameshift mutations, or contained a mutant start codon retained Cas13 inhibition (Fig. 1B and fig. S1B). When we analyzed the transcriptional products of the Acr constructs using small RNA sequencing, we detected reads corresponding to RNAs between 37 and 60 nucleotides (nt) in length, which mapped to the reverse strand of the intergenic region upstream of *acrVIA2* (Fig. 1C). We identified putative -10 and -35 elements of a reverse-facing promoter downstream of the small RNA transcriptional start site (Fig. 1A), which we found to be essential for Cas13 inhibition (Fig. 1B). We confirmed the Acr-specific production of a 60-nt RNA matching this region using Northern blot (Fig. 1D). These results suggest that a small RNA divergently transcribed from *acrVIA2* acts as a Cas13 inhibitor. On the basis of the following analysis, we refer to this factor as rAcrVIA1, in accordance with recently established nomenclature

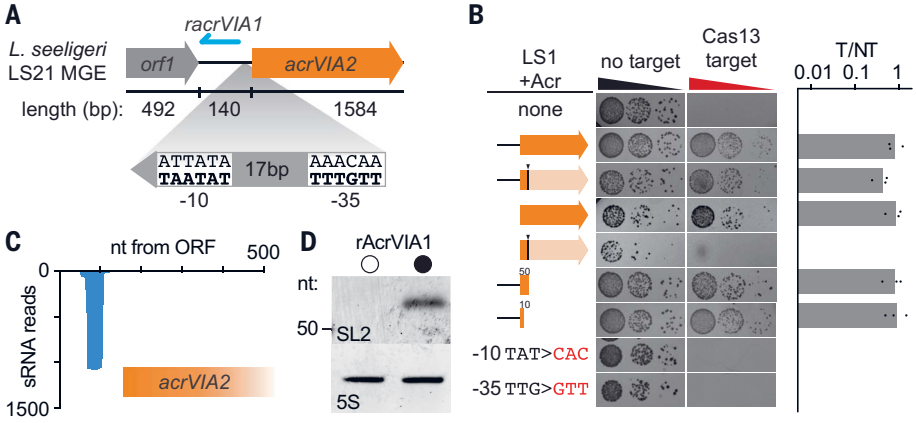

Fig. 1. A small noncoding RNA (rAcrVIA1) inhibits type VI CRISPR interference. (**A**) Schematic of genetic locus encoding AcrVIA2 (orange) and rAcrVIA1 (blue) found in integrated plasmid of *L. seeligeri* strain LS21. Predicted promoter -10 and -35 elements driving rAcrVIA1 transcription. (**B**) Plasmid targeting assay demonstrating Cas13 inhibition. Conjugative plasmids expressing a Cas13 target (or not) were introduced into *L. seeligeri* strains harboring the indicated Acr constructs. Black arrows and lines indicate nonsense mutations. Numbers indicate number of *acrVIA2* coding DNA sequence (CDS) nucleotides left after truncation. Quantification of three biological replicates is shown. T/NT, ratio of transconjugants observed with target plasmid to that with nontarget plasmid. (**C**) Small RNA (sRNA) sequencing reads mapped to the racrVIA1 locus when expressing *racrVIA1-acrVIA2* in strain LS1. Combined reads from two biological replicates are shown. (**D**) Northern blots using probe antisense to *racrVIA1* or 5S ribosomal RNA (rRNA).

[1]Department of Microbiology, University of Washington, Seattle, WA, USA. [2]Department of Biochemistry, SUSTech Homeostatic Medicine Institute, School of Medicine, Southern University of Science and Technology, Shenzhen, Guangdong, China. [3]Shenzhen Key Laboratory of Cell Microenvironment, Guangdong Provincial Key Laboratory of Cell Microenvironment and Disease Research, Key University Laboratory of Metabolism and Health of Guangdong, Institute for Biological Electron Microscopy, Southern University of Science and Technology, Shenzhen, Guangdong, China.
*Corresponding author. Email: meeske@uw.edu (A.J.M.); jian@sustech.edu.cn (N.J.)
†These authors contributed equally to this work.

for rAcrs (*2*). However, unlike previously described rAcrs, rAcrVIA1 does not bear sequence homology to type VI crRNAs (fig. S1, C and D). In contrast to its effects on type VI CRISPR immunity, rAcrVIA1 did not affect plasmid interference by the DNA-targeting type II-A or II-C CRISPR systems of *L. seeligeri*, although we observed modest yet reproducible inhibition of type I-B CRISPR immunity (fig. S1E).

Secondary structural features of rAcrVIA1 are required for Cas13 inhibition

Secondary structure prediction of rAcrVIA1 using RNAfold (*4*) suggests it forms two stem loops (SLs) with a 2-nt bulge in SL1, similar to that formed by crRNA (Fig. 2A and fig. S2A) (*5*). To test the contribution of these predicted structural features to Cas13 inhibition, we generated a series of mutant rAcrVIA1 alleles. First, we found that removal of either SL abolished Cas13 inhibition by rAcrVIA1 (fig. S2B). We observed similarly strong requirements for specific base pairs within each SL, as disruption of complementarity at 2 or 3 bp eliminated rAcrVIA1 activity (Fig. 2B). Furthermore, restoration of complementarity by compensatory mutation of the other strand of the SL rescued rAcrVIA1-mediated inhibition of Cas13 in both cases, validating the formation of these predicted base pairs and underscoring the importance of the stem structure (but not the sequence) for Cas13 inhibition. Next, we investigated the contributions of various predicted structural features in rAcrVIA1 to its inhibitory activity (fig. S2, A and B). Shortening the length of either SL by 1 bp largely eliminated rAcrVIA1 activity, as did lengthening SL1 by 1 bp. By contrast, lengthening SL2 by 1 bp had no effect on rAcrVIA1-mediated Cas13 inhibition.

Cas13 interacts with rAcrVIA1

Next, we investigated the mechanism of Cas13 inhibition by rAcrVIA1. To test whether rAcrVIA1 physically associates with Cas13, we coexpressed a functionally tagged plasmid-borne dCas13-his6 allele and CRISPR array harboring a single spacer, along with rAcrVIA1, mutant derivatives, or an empty vector control in a ΔCRISPR-Cas13 mutant strain of *L. seeligeri* (Fig. 2, C and D). We used nuclease-inactive dCas13 to avoid confounding effects from potential RNA cleavage products. We then affinity purified dCas13-his6 from both strains by nickel–nitrilotriacetic acid agarose pulldown, extracted RNA from the purified protein, and analyzed dCas13-associated RNAs by denaturing gel electrophoresis. In the absence of rAcrVIA1, we detected two bands corresponding to the expected 50- to 51-nt crRNA normally associated with dCas13 (Fig. 2C). However, in the presence of rAcrVIA1, we observed an additional 60-nt RNA, along with diminished intensity of the crRNA bands. We performed similar experiments with an *apo* form of dCas13 lacking a CRISPR array, which resulted in coprecipitation of Cas13 with mature rAcrVIA1 but no crRNA (Fig. 2C). We determined using small RNA sequencing that the 60-nt band bound to *apo*-dCas13 corresponded to the rAcrVIA1 sequence (Fig. 2D). These results indicate that rAcrVIA1 physically interacts with Cas13 in a manner that does not require the presence of crRNA and suggest that rAcrVIA1 competes with crRNA for binding to Cas13. To investigate this, we tested whether Cas13 immunity could be rescued from rAcrVIA1-mediated inhibition by overexpressing crRNA, through ectopic integration of a copy of the CRISPR array under a strong P_{hyper} promoter. When we challenged this strain with a CRISPR-targeted plasmid, we observed reduced numbers and size of transconjugant colonies, consistent with much weaker rAcrVIA1 activity (Fig. 2B). Cas13 is responsible for processing type VI-A crRNAs (*6*), raising the possibility that it could also process rAcrVIA1 precursors. Consistent with this idea, we observed no coimmunoprecipitation of rAcrVIA1 (or crRNAs) with a mutant allele of dCas13 lacking crRNA processing activity (R1048A and K1049A) (Fig. 2C) (*5*); however, this mutant could be impaired in binding of crRNAs and/or rAcrVIA1.

We then performed dCas13 pulldowns in the presence of the mutant rAcrVIA1 derivatives tested (fig. S2C). Whereas wild-type (WT) rAcrVIA1 and all of the mutant alleles that retained Cas13 inhibition coimmunoprecipitated with dCas13, several of the mutants that lost function failed to associate with dCas13. Notably, although the SL2 Δ1bp mutant largely lost the ability to inhibit Cas13, it remained associated with dCas13, suggesting that the interaction between rAcrVIA1 and Cas13 is necessary but may be insufficient for inhibition. However, this mutant resulted in the formation of numerous small target plasmid–containing transconjugant colonies, suggesting that it retains partial function (fig. S2B, asterisk). That rAcrVIA1 interacts with Cas13 raised the possibility that rAcrVIA1 itself functions as a crRNA. Accordingly, we tested whether a

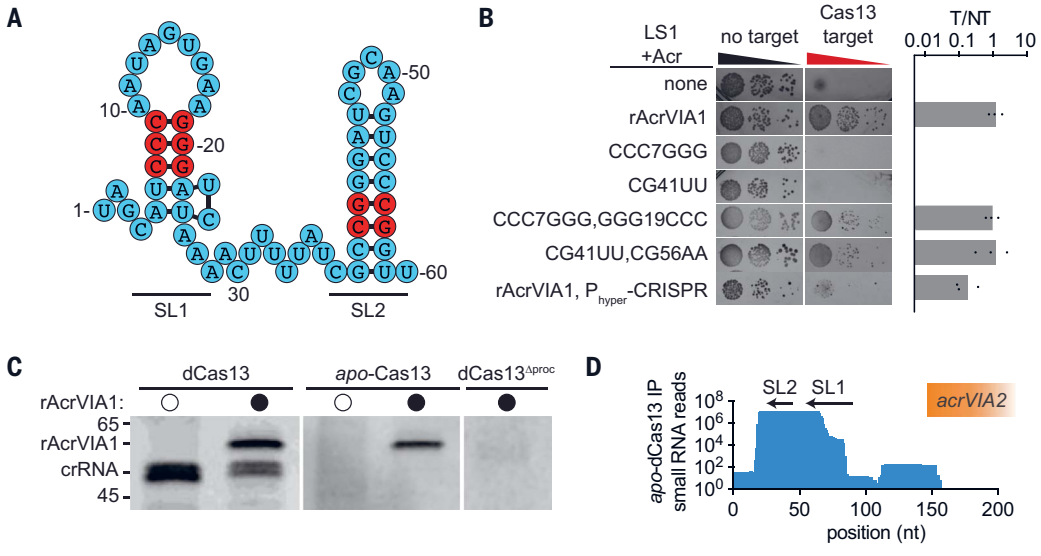

Fig. 2. Secondary structure, processing, and Cas13-binding activity of rAcrVIA1. (**A**) Predicted secondary structure of rAcrVIA1, with SLs (SL1 and SL2). Red nucleotides indicate positions mutated in (B). (**B**) Plasmid-targeting assay demonstrating that mutations in each SL abolish Cas13 inhibition, whereas compensatory mutations that restore complementary rescue inhibition. Quantitation of three biological replicates. (**C**) Denaturing gel analysis of RNA associated with the indicated Cas13 allele in the presence or absence of rAcrVIA1. RNA molecular weight markers in nucleotides. (**D**) sRNA sequencing reads mapping to *racrVIA1* locus from RNA extracted from purified apo-dCas13 in the presence of rAcrVIA1. IP, immunoprecipitation.

plasmid encoding a transcript complementary to rAcrVIA1 was restricted in the presence of rAcrVIA1 or a mutant in which SL2 was disrupted to allow target RNA engagement (fig. S2D). We observed no rAcrVIA1-dependent restriction with either construct and argue that the rAcr does not function as a crRNA, which may be explained by sequence differences in the crRNA handle (SL1) portion.

Cryo–electron microscopy structure of the Cas13-rAcrVIA1 complex

To investigate the mechanism of rAcrVIA1-mediated Cas13 inhibition, we coproduced *apo*-Cas13 with rAcrVIA1 in *L. seeligeri*. Size exclusion chromatography analysis demonstrated the formation of a homogeneous complex between Cas13 and rAcrVIA1 (fig. S3A). We determined its cryo–electron microscopy (cryo-EM) structure at a resolution of 2.85 Å (Fig. 3, A and B, and fig. S3, B to F). The Cas13-rAcrVA1 complex adopts a bilobed architecture, consisting of recognition [N-terminal domain (NTD) and helical-I domain] and nuclease [helical-II and two higher eukaryotes and prokaryotes nucleotide-binding (HEPN) domains connected by a linker element] lobes. Notably, we observed RNA densities corresponding to

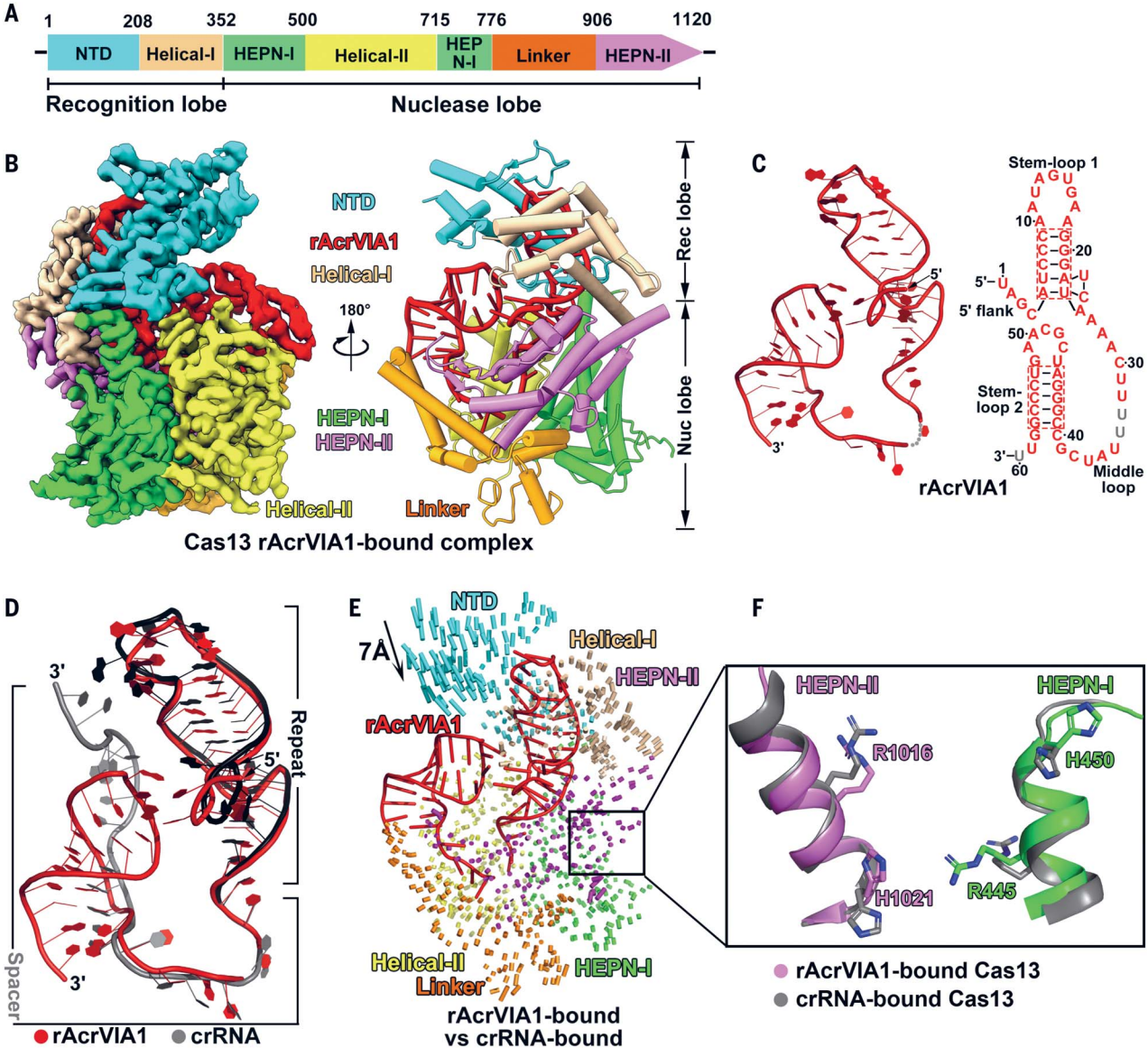

Fig. 3. Overall architecture of the Cas13-rAcrVIA1 complex. (**A**) Domain organization of Cas13. (**B**) Surface (left) and ribbon (right) representation of the cryo-EM structure of Cas13-rAcrVIA1 complex in different orientations. Domains are colored as in (A). (**C**) Ribbon representation (left) and schematic drawing (right) of the sequences and secondary structure of rAcrVIA1. Segments that could be traced are in color, and disordered segments are in gray. (**D**) Structural comparison of Cas13-bound rAcrVIA1 (red) and crRNA (gray). The repeat and spacer regions of the crRNA are colored in black and gray, respectively. (**E**) Structural comparison of Cas13-rAcrVIA1 complex and the Cas13-crRNA complex. The vector length correlates with the scale of domain movement. Domains are colored as in (A). (**F**) Comparison of the positions of the four catalytic residues from HEPN-I and HEPN-II domains between rAcrVIA1-bound and crRNA-bound Cas13. Single-letter abbreviations for the amino acid residues are as follows: A, Ala; C, Cys; D, Asp; E, Glu; F, Phe; G, Gly; H, His; I, Ile; K, Lys; L, Leu; M, Met; N, Asn; P, Pro; Q, Gln; R, Arg; S, Ser; T, Thr; V, Val; W, Trp; and Y, Tyr.

the 60-nt rAcrVIA1, which consists of two SLs (SL1: A5-U25; SL2: C41-G57), a 4-nt 5′ flank (U1-C4), and a 15-nt middle loop (A26-C40) (Fig. 3C). The 5′ flank protrudes from SL1 and inserts into a surface-exposed groove formed by the helical-I and HEPN-II domains (Fig. 3B and fig. S4A). The 5′ hydroxyl group of U1 is anchored near the conserved residues R1041, R1048, and K1051, which are responsible for crRNA maturation (fig. S4B) (*5*, *7*), suggesting that the 5′ end of rAcrVIA1 might be processed similarly to mature crRNA. The 3′ end of rAcrVIA1 is exposed to the solvent (Fig. 3B and fig. S4C), suggesting a potential alternative nuclease-mediated processing mechanism for this region.

SL1 is stabilized primarily through sequence-independent interactions with the NTD and helical-I domains (fig. S4D). Nucleotides A5 and U6 base pair with U25 and A22, respectively, forming a 2-nt bulge (U23 and C24), as in crRNA bound to *L. seeligeri* Cas13 (fig. S4E) (*5*). The middle loop undergoes a 90° turn and is positioned in the crRNA-target RNA binding channel through sequence-independent interactions mediated by the HEPN-II, helical-II, and linker domains (fig. S4, D and F). SL2, adopting an A-form helical conformation, is situated in the cleft formed by NTD and linker domains (Fig. 3B). Few interactions are involved in maintaining the structure of SL2, including nucleotide G48 stacking with residues K306 in the helical-I domain and nucleotides G48, A50, and A51 stacking with nucleotides C4 and G3 of the 5′ flank (fig. S4D). Consistent with our mutagenesis experiments, these structural analyses indicate that Cas13 binds rAcrVIA1 in a shape-dependent rather than sequence-dependent manner. Next, we superimposed the Cas13-rAcrVIA1 complex with the Cas13-crRNA complex. The structure of rAcrVIA1 closely resembles that of crRNA, except for the differences in their 3′ region (Fig. 3D). Whereas the 3′ end of crRNA extends outward and inserts into the NTD domain (fig. S4G) (*5*), rAcrVIA1 forms a SL structure that sits in the cleft between NTD and linker domains (Fig. 3B), similar to the structure formed by crRNA bound to *Leptotrichia buccalis* Cas13 (fig. S4H) (*7*). When Cas13 binds to rAcrVIA1, its structure undergoes minor rearrangements compared with its crRNA-bound form, with a Cα root mean square deviation value of 1.9 Å over 865 atoms (Fig. 3E). Notably, upon binding rAcrVIA1, the NTD domain of Cas13 shifts nearly 7 Å toward the helical-I domain, forming a narrow cleft to accommodate SL2 (Fig. 3E).

We compared the conserved HEPN catalytic site of the rAcrVIA1-bound *L. seeligeri* Cas13 with the crRNA-bound form, which revealed minimal conformational changes in the catalytic ribonuclease residues (Fig. 3F). These catalytic sites have been shown to undergo substantial conformational changes upon target RNA binding to perform RNA cleavage (fig. S4I) (*7*). Because Cas13-rAcrVIA1 cannot bind target RNA, rAcrVIA1 effectively locks Cas13 in a catalytically inactive state. Structural analysis using a protein-ligand interaction profiler tool indicated that rAcrVIA1 and crRNA form a similar number of hydrogen bond interactions with Cas13 (76 hydrogen bonds for rAcrVIA1 and 72 hydrogen bonds for crRNA) (*8*). To further assess the binding ability of rAcrVIA1 and crRNA to Cas13, we incubated fluorescently labeled rAcrVIA1 and crRNA with increasing concentrations of the Cas13-rAcrVIA1 complex. The results showed that both rAcrVIA1 and crRNA bind to Cas13 with similar affinities (fig. S5), consistent with our in vivo observations that overexpression of crRNA can rescue rAcrVIA1-mediated Cas13 inhibition (Fig. 2B). Taken together, these findings suggest that rAcrVIA1 mimics the structure of crRNA and competes with it for binding, thereby preventing Cas13 from recognizing and cleaving target RNA.

AcrVIA2 and rAcrVIA1 contribute independently to Cas13 inhibition

AcrVIA2 is encoded downstream of rAcrVIA1 and inhibits type VI CRISPR immunity by affecting crRNA levels, either by mediating their direct cleavage or by enabling their degradation by other nucleases (Fig. 4A) (*3*). Thus, both rAcrVIA1 and AcrVIA2 affect crRNA:Cas13 stoichiometry, suggesting they may synergize in Cas13 inhibition. To investigate this possibility, we analyzed dCas13-associated RNA during expression of rAcrVIA1, AcrVIA2, or both factors (Fig. 4B). As previously demonstrated, AcrVIA2 expression resulted in reduced crRNA levels but did not affect dCas13 levels. During rAcrVIA1 expression, bands corresponding to both crRNA and rAcrVIA1 were detected in the dCas13-bound RNA fraction. When we coexpressed rAcrVIA1 and AcrVIA2, the rAcrVIA1 band represented the predominant dCas13-bound RNA, indicating the activities of rAcrVIA1 and AcrVIA2 are not mutually exclusive, and despite its mimicry of crRNA, rAcrVIA1 is not susceptible to AcrVIA2-mediated degradation.

During natural invasion of *L. seeligeri* by mobile genetic elements (MGEs) encoding rAcrVIA1 and AcrVIA2, the cell would presumably be equipped with active Cas13 ribonucleoprotein (RNP) complexes available for target RNA recognition before either Acr is expressed, making immunity difficult to suppress. To model this scenario, we introduced type VI spacers, recognizing the kanamycin resistance mRNA encoded on the same conjugative plasmid harboring rAcrVIA1, AcrVIA2, or both, and measured conjugation efficiency (Fig. 4C). Whereas expressing AcrVIA2 alone had a negligible ability to suppress Cas13 targeting, expressing rAcrVIA1 or both Acrs completely inhibited Cas13, suggesting rAcrVIA1 is capable of neutralizing immunity during natural invasion of *L. seeligeri* equipped with preexisting Cas13 targeting complexes. In support of this hypothesis, preincubation of Cas13-crRNA with a molar excess of rAcrVIA1 inhibited target RNA cleavage in vitro (Fig. 4D).

Regulatory control of rAcrVIA1

The rAcrVIA1 locus is naturally found immediately downstream of another gene (*orf1*), encoding a protein with a predicted helix-turn-helix (HTH) domain (Fig. 4A). Thus, we sought to investigate whether this gene affects rAcrVIA1 function. We cloned the locus from the native *orf1* promoter through the *acrVIA2* gene, which abolished Cas13 interference in plasmid-targeting assays (Fig. 4E). Furthermore, AcrVIA2 was dispensable for Cas13 inhibition, suggesting that rAcrVIA1 is functional in this construct. Next, we tested an in-frame deletion of *orf1*, which had no impact on Cas13 inhibition when both *racrVIA1* and *acrVIA2* remained intact. When we deleted *orf1* from the construct solely expressing rAcrVIA1, Cas13 inhibition was abolished and could be rescued by the expression of *orf1* in *trans*. We observed a similar loss of rAcr function when we installed an early nonsense mutation in *orf1*, disrupting ORF1 function but preserving sequence architecture. A construct expressing *orf1* alone did not affect Cas13 activity, suggesting ORF1 is not itself an Acr. Because rAcrVIA1 is functional in the absence of both *orf1* and its promoter (P_{orf1}), we tested whether mutating P_{orf1} could relieve the requirement of ORF1 for rAcrVIA1 function. Indeed, ablation of the predicted P_{orf1}-10 element restored Cas13 inhibition by rAcrVIA1 in the absence of *orf1*. As ORF1 is a predicted nucleic acid–binding protein, we investigated whether it influences rAcrVIA1 activity by affecting the transcriptional activity of its own promoter (P_{orf1}). We ectopically integrated a transcriptional fusion of this promoter to the fluorescent protein mStayGold into the LS1 chromosome and measured fluorescence in the presence and absence of a plasmid encoding ORF1 (Fig. 4F). Whereas we observed strong reporter activity from P_{orf1} alone, the addition of ORF1 reduced the activity by 100-fold, similar to the levels observed after ablation of the P_{orf1}-10 element, indicating that ORF1 is a transcriptional autorepressor. We hypothesized that P_{orf1} drives strong transcription that conflicts with the convergently transcribed rAcrVIA1; thus, rAcrVIA1 can only be produced when P_{orf1} is silenced by ORF1. To investigate this, we generated an mStayGold reporter to measure P_{orf1}-driven readthrough transcription downstream of the *orf1* stop codon, antisense with respect to rAcrVIA1 (Fig. 4F). The reporter construct

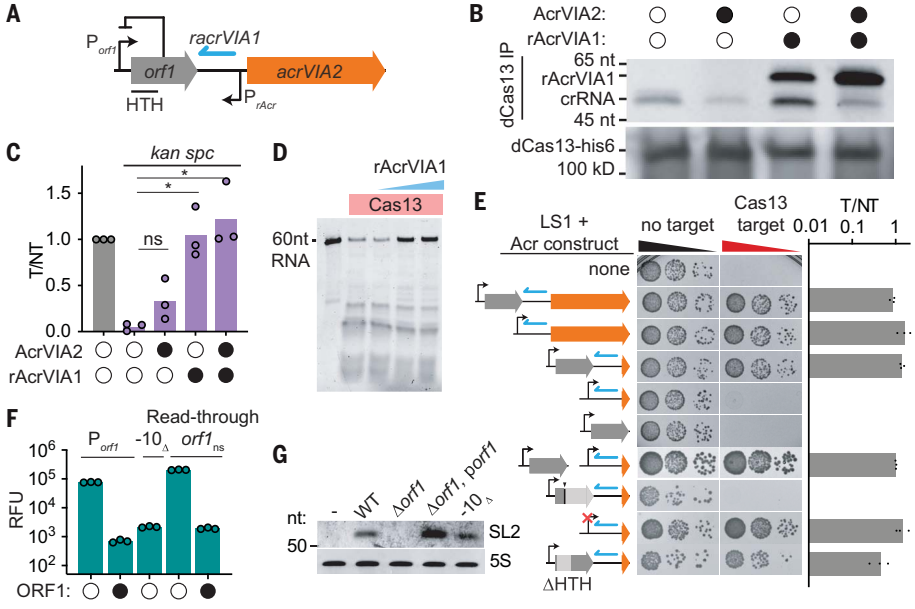

Fig. 4. rAcrVIA1 acts independently of AcrVIA2 and is regulated by ORF1. (**A**) Schematic of genetic locus encoding HTH-containing ORF1, rAcrVIA1, and AcrVIA2. (**B**) (Top) Analysis of dCas13-associated RNA in presence of the indicated Acrs. (Bottom) dCas13-his6 Western blot. (**C**) Plasmid-targeting assay in which plasmids encoding Acrs were directly targeted by preexisting Cas13 RNP complexes. Acr plasmids were conjugated into strain LS1 with or without a targeting spacer, and transconjugants were enumerated. T/NT, targeted to nontargeted transconjugants ratio. Quantification of three biological replicates. Asterisks indicate statistical significance ($P < 0.05$, Student's t test). ns, not significant. (**D**) RNA cleavage assay with purified 3xFlag-tagged Cas13-crRNA and Cy3-labeled target RNA substrate, with rAcrVIA1 added in 1:8, 1:2, and 2:1 molar ratios. Representative of three biological replicates. (**E**) Plasmid-targeting assay. Conjugative plasmids expressing a Cas13 target (or not) were introduced into *L. seeligeri* strains harboring the indicated Acr constructs. Quantification of three biological replicates. (**F**) Transcriptional activity of the indicated promoters in the presence and absence of ORF1. RFU, relative fluorescence units. (**G**) Northern blots using probes antisense to rAcrVIA1 or 5S rRNA sequence.

contained an early nonsense mutation in *orf1* to prevent silencing. Using this reporter, we observed strong transcriptional activity downstream of *orf1*, which was silenced when ORF1 was supplied in *trans* (Fig. 4F). We found that rAcrVIA1 levels were undetectable by Northern blot when *orf1* was mutated in the presence of P_{orf1} but were restored upon mutation of the P_{orf1}-10 element or by expressing ORF1 in *trans*, indicating that convergent transcription from P_{orf1} interferes with rAcrVIA1 production (Fig. 4G). Deletion of the ORF1 HTH only weakly affected rAcrVIA1 activity in plasmid-targeting assays, indicating that it is not strictly required for rAcrVIA1 production (Fig. 4E). Taken together, our results indicate that ORF1 is a transcriptional autorepressor whose activity is required to repress convergent transcription that influences rAcrVIA1 production.

Discussion

Our analyses support the conclusion that rAcrVIA1 is a structural mimic of type VI crRNA that inhibits Cas13 by competing with crRNA for Cas13 binding. Previously described rAcrs share a high degree of sequence homology with the crRNAs of their cognate CRISPR types (*2*). By contrast, rAcrVIA1 has negligible sequence similarity to type VI crRNA, yet the two RNAs adopt a notably similar fold. Our results suggest there may be more structural mimic rAcrs or RNA inhibitors of other defense systems to be discovered, yet their identification poses a challenge to homology-based bioinformatic approaches. Accordingly, few examples of RNA-based structural mimicry in immune antagonism have been identified. One parallel mechanism in viral counter defense against eukaryotic immunity is the adenoviral RNA VAI, a double-stranded RNA that mimics the natural substrate of the immune sensor protein kinase R (PKR) (*9*). VAI functions as a pseudoactivator, binding PKR and inhibiting rather than stimulating its immune activities.

Why is rAcrVIA1 encoded just upstream of another Cas13 inhibitor, AcrVIA2? This arrangement is paralleled for several rAcrs, which are encoded alongside protein-based inhibitors of the same CRISPR type (*2*). Although in all cases tested so far, the RNA and protein Acrs can function independently when produced in advance of CRISPR targeting, our experiments demonstrated that rAcrVIA1 functions more efficiently during initial invasion by the MGEs that encode it. We speculate that rAcrs may serve to neutralize preexisting CRISPR-Cas complexes, and their cognate protein Acrs such as AcrVIA2 serve to maintain immune suppression by inhibiting biogenesis of new CRISPR machinery.

REFERENCES AND NOTES

1. J. Bondy-Denomy, A. Pawluk, K. L. Maxwell, A. R. Davidson, *Nature* **493**, 429–432 (2013).
2. S. Camara-Wilpert *et al.*, *Nature* **623**, 601–607 (2023).
3. M. A. Katz *et al.*, *Nature* **634**, 677–683 (2024).
4. R. Lorenz *et al.*, *Algorithms Mol. Biol.* **6**, 26 (2011).
5. A. East-Seletsky *et al.*, *Nature* **538**, 270–273 (2016).
6. A. J. Meeske *et al.*, *Science* **369**, 54–59 (2020).
7. L. Liu *et al.*, *Cell* **170**, 714–726.e10 (2017).
8. M. F. Adasme *et al.*, *Nucleic Acids Res.* **49**, W530–W534 (2021).
9. M. G. Katze, D. DeCorato, B. Safer, J. Galabru, A. G. Hovanessian, *EMBO J.* **6**, 689–697 (1987).

ACKNOWLEDGMENTS

We are grateful to all members of the Meeske and Jia laboratories for helpful discussions. We thank the staff at Southern University of Science and Technology (SUSTech) Cryo-EM Center for assistance in data collection on the SUSTech Titan KRIOS cryo-EM. **Funding:** This study received support from the National Institutes of Health (grant R35GM142460 to A.J.M.); the National Science Foundation (grant FAIN2235762 to A.J.M.); the Rita Allen Foundation (to A.J.M.); the National Natural Science Foundation of China (32270050 to N.J.); a Guangdong Provincial Science and Technology Innovation Council grant (2017B030301018 to N.J.); and the SUSTech Institute for Biological Electron Microscopy (to N.J.). **Author contributions:** Conceptualization: A.J.M., N.J.; Cryo-EM sample preparation; data collection, processing, and analysis; and structure refinement: J.-T.Z.; Genetics and pulldown experiments: V.M.H., M.A.K., B.K., A.J.M.; Protein purification: J.-T.Z., Y.L., D.M.B.; Writing – original draft: A.J.M., N.J.; Writing – review & editing: V.M.H., J.-T.Z., M.A.K., Y.L., B.K., D.M.B., N.J., A.J.M. **Competing interests:** A.J.M. is a cofounder of Profluent Bio. The other authors declare that they have no competing interests. **Data and materials availability:** The cryo-EM density map of Cas13-rAcrVIA1 complex has been deposited in the Electron Microscopy Data Bank (EMDB) under accession number EMD-60476. The atomic coordinate of Cas13-rAcrVIA1 complex has been deposited in the Protein Data Bank (PDB) with accession number 8ZTY. All other data are available in the main text or the supplementary materials.

SUPPLEMENTARY MATERIALS

science.org/doi/10.1126/science.adr3656
Materials and Methods
Figs. S1 to S5
Table S1
References (*10*–*23*)
MDAR Reproducibility Checklist
Data S1 to S5

Submitted 27 June 2024; accepted 7 March 2025
10.1126/science.adr3656